ISBN: 978-3-95450-247-9 ISSN: 2673-5490 doi: 10.18429/JACoW-IPAC2024-MOPC34

PERFORMANCE TEST FOR SINGLE-SPOKE RESONATOR SUPERCONDUCTING CAVITIES IN RAON

H. Kim, J. Kim, J. Lee, M. Kim, H. Park, Y. Jung†, Institute for Rare Isotope Science, Institute for Basic Science, Daejeon, Republic of Korea
S. Jeon, Department of Physics, Kyungpook National University, Daegu, Republic of Korea

Abstract

Single-spoke resonators (SSRs) have been developed and tested for the RAON SCL2 project. The design parameters for the SSRs are provided, and the performance of the superconducting cavities is assessed. The single-spoke resonator cavities, cryogenic systems, cryostats, and human machine interface (HMI) are depicted for a vertical test. Calibration and cavity preparations are demonstrated to evaluate the performance of the superconducting cavities. Testing of the single-spoke resonator type 1 (SSR1) performance is conducted via a vertical test. Q slopes are presented as a function of accelerating field, and Lorentz force detuning (LFD) as well as pressure sensitivity are conducted for the superconducting cavities.

INTRODUCTION

Superconducting cavities have undergone extensive development, resulting in a variety of types used in accelerators. Field emission phenomena have been thoroughly studied and applied to superconducting cavities [1, 2, 3]. Techniques for measuring quality factors in superconducting cavities have been investigated, and the conservation of quality factors has been applied to both superconducting cavities and mammalian studies [4, 5]. Quarter-wave resonator (QWR) and half-wave resonator (HWR) cavities have been developed, installed, and commissioned for beam operation at the RAON superconducting linear accelerator 3 (SCL3) site [6, 7]. This study focuses on the performance of single-spoke resonator SSR1 cavities, presenting their design parameters and characteristics. Cryogenic systems, cryostats, and HMI are depicted for the vertical test. Quality factor, Lorentz force detuning (LFD), and pressure sensitivity are among the parameters measured.

PREPARATION FOR TEST

Single-spoke resonator (SSR) cavities have been developed, fabricated, and tested for the RAON SCL2 project. The SSR cavities consists of type 1 (SSR1) and type 2 (SSR2).

Table 1 displays the design parameters for SSR1 and SSR2 cavities. The drive frequency for SSR1 and SSR2 is 325 MHz, with the optimum β (v/c) being 0.3 for SSR1 cavity and 0.51 for SSR2 cavity.

Table 1: Parameters for the Single-Spoke Resonator (SSR) Cavities

Parameter	SSR1	SSR2
β_{OPT}	0.3	0.51
f (MHz)	325	325
$L_{eff}(=\beta_0\lambda)(mm)$	276.9	470.8
R/Q (Ω)	233	290
E_{peak}/E_{acc}	4.1	3.7
B_{peak}/E_{acc} [mT/(MV/m)]	6.9	7.7
E_{acc} (MV/m)	8.5	8.7
V_{acc} (MV)	2.35	4.1
Stored energy (J)	11.6	28.3
QR_s	92.2	112.9
kappa	55.13	36.17

Figure 1 depicts the images of the single-spoke resonators (SSRs). The SSR cavities are prepared for vertical testing and can be shielded with mumetal.

The surface resistance of the superconducting cavities can be described by the equation:

$$R_s = R_{BCS} + R_{res} + R_{mag} \quad (1)$$

Here, R_s represents the surface resistance, R_{BCS} is the BCS resistance, R_{res} is the residual resistance, and R_{mag} is the magnetic field resistance.

The magnetic field resistance (R_{mag}) due to magnetic shielding can be approximated as follows [8]:

$$R_{mag} = 1.94 \times 10^{-4} \sqrt{\frac{f[Hz]}{RRR}} H_0(\mathrm{m}G)\ [\mathrm{n}\Omega] \quad (2)$$

where f is the frequency in Hertz, RRR is the residual resistivity ratio, and H_0 is the magnetic field strength in milligauss (mG).

* This work was supported by the National Research Foundation of Korea (NRF) funded by the Ministry of Science and ICT (RS-2022-00214790).
† sulsiin@ibs.re.kr

ISBN: 978-3-95450-247-9 ISSN: 2673-5490 doi: 10.18429/JACoW-IPAC2024-MOPC34

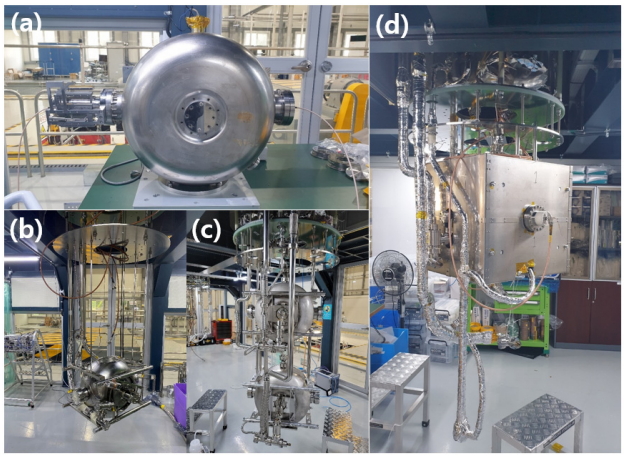

Figure 1: Images of single-spoke resonators (SSRs). (a) SSR cavity with jacket, (b) SSR cavity without jacket, (c) SSR cavities with jackets, and (d) SSR cavity with magnetic shielding.

For single-spoke resonator (SSR) cavities with an RRR of 300 and a frequency of 325 MHz, Table 2 presents the surface resistance versus magnetic shielding field for SSR cavities. The magnetic shielding field is maintained below 10 mG, which corresponds to a surface resistance of 2 nΩ.

Table 2: Surface Resistance vs. Magnetic Shielding Field

Magnetic field, H(mG)	**Surface resistance, R_{mag}(nΩ)**
1	0.2
2	0.4
5	1
10	2
20	4
30	6
40	8
50	10

VERTICAL TEST

Figure 2 displays the cryogenic system and cryostat. The cryogenic system comprises a helium liquefier with a capacity of 280 L/h, a liquid helium dewar with a capacity of 3,000 L, warm pumps for 2 K pumping at a rate of 1.5 g/s per warm pump, recovery compressors, gas bags, and a liquid nitrogen tank. The cryostat includes a 4 K helium reservoir, a 2 K helium reservoir, cryogenic valves, vacuum lines for cavity pumping, and superconducting test cavities. Cavity pumping is achieved using dry pumps, turbo molecular pumps (TMP), and ion pumps.

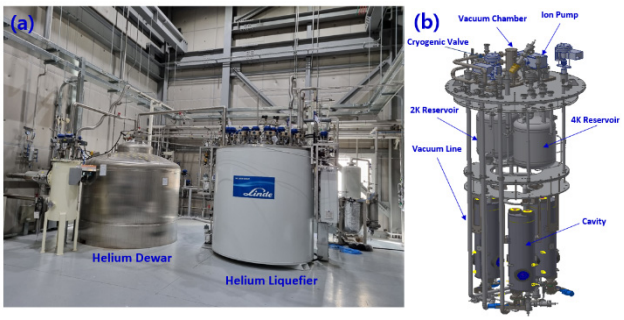

Figure 2: Cryogenic system and cryostat. (a) helium liquefier and helium dewar, and (b) cryostat.

Liquid nitrogen is supplied first, followed by liquid helium to cool down the superconducting cavities. Calibration is performed once the cavity temperature reaches 4.2 K.

RF conditioning lasts for approximately 5 hours, and the multipacting (MP) conditioning range varying from 0.5 to 4 MV/m depending on the cavity. Field emission conditioning occurs at accelerating fields higher than those that cause X-ray generation from field emission on the cavity surface. After field emission conditioning, the Q factor increases, and X-ray generation decreases.

In many cases, the field emission conditioning leads to an increase in cavity vacuum pressure, potentially altering the shape or curvature of particles by melting the tips on the RF surfaces.

The field emission conditioning near the maximum accelerating field is effective for the first three attempts using continuous wave (CW) or pulsed RF. However, the effect of the field emission conditioning becomes negative when attempted more than four times, either at 4.2 K or 2 K.

Figure 3 shows the images for control panels of vertical test. Spectrum analyzer, low level radio frequency (LLRF) test panel, RF control panel, and cryostat monitor are used to the vertical test.

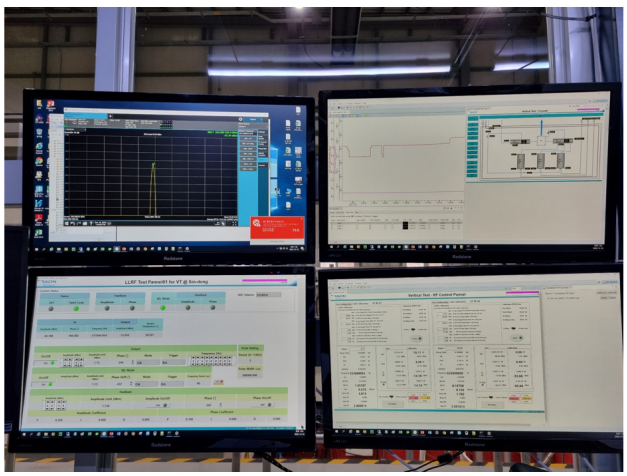

Figure 3: Images of control panels for the vertical test. Spectrum analyzer, LLRF test panel, RF control panel, and cryostat monitor are shown.

ISBN: 978-3-95450-247-9 ISSN: 2673-5490 doi: 10.18429/JACoW-IPAC2024-MOPC34

Figure 4 displays the Q factor as a function of accelerating field for single-spoke resonator SSR1 cavities. X-ray radiation begins to be generated at 5.4 MV/m for SSR1 VZ#2 and at 6.2 MV/m for SSR1 VZ#3. The Q factor for each cavity remains higher than the reference value of 3.2×10^9 at 8.5 MV/m.

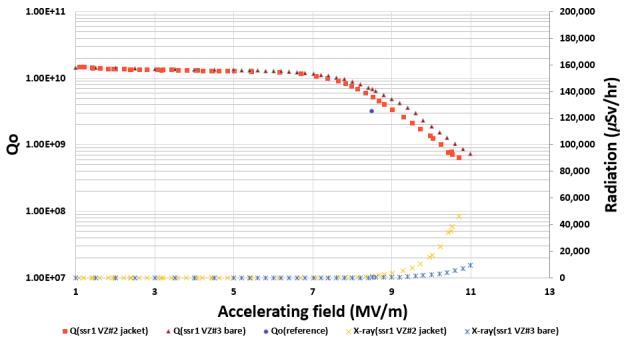

Figure 4: Q factor as a function of the accelerating field for SSR1 cavities. The slope of the Q factor curve is measured for SSR1 VZ#2 and VZ#3 cavities.

Figure 5 illustrates the measurement of Lorentz force detuning (LFD) for an SSR2 cavity. The LFD is recorded as -26.4 Hz/(MV/m)^2 for the SSR1 VZ#2.

Additionally, the LFD is measured as -12.3 Hz/(MV/m)^2 for the jacket of SSR1 VZ#1. The LFD of the SSR1 VZ#1 jacket is lower than that of the SSR1 VZ#2 jacket.

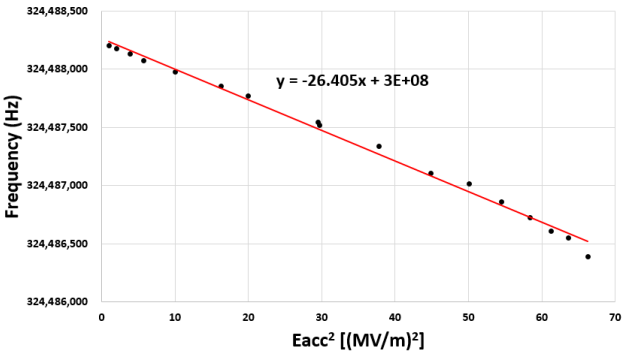

Figure 5: Measurement of the Lorentz force detuning (LFD) for an SSR1 cavity. The Lorentz force detuning (LFD) is recorded as -26.4 Hz/(MV/m)^2 for the SSR1 VZ#2 jacket.

Figure 6 illustrates the pressure sensitivity measurement for an SSR1 cavity. The pressure sensitivity is determined at an accelerating field of 2 MV/m while maintaining critical coupling by adjusting a variable coupler. This is achieved by gradually pumping the vapour pressure of liquid helium from 1013 mbar down to 25 mbar. The amplitude of the RF power, the phase of the low-level radio frequency (LLRF), and the pulse of the variable coupler are adjusted to maintain the accelerating field and critical coupling. The resonance frequency of the cavity is measured during the cooling-down process. Pressure sensitivity data is collected for the pressure range between 25 and 170 mbar. The measured pressure sensitivity is recorded as -523.9 Hz/mbar for the SSR1 VZ#2 jacket. The relatively high measured pressure sensitivity is attributed to the cavity not being securely fixed, resulting in an almost free boundary condition during the vertical test.

Additionally, the pressure sensitivity is measured as -27.9 Hz/mbar for the SSR1 VZ#1 jacket. During the pressure sensitivity measurement of the SSR1 VZ#1 jacket, the cavity is tightly fixed, resembling a fixed boundary condition, during the vertical test. This condition includes the application of a tuner force on the cavity, which is roughly considered.

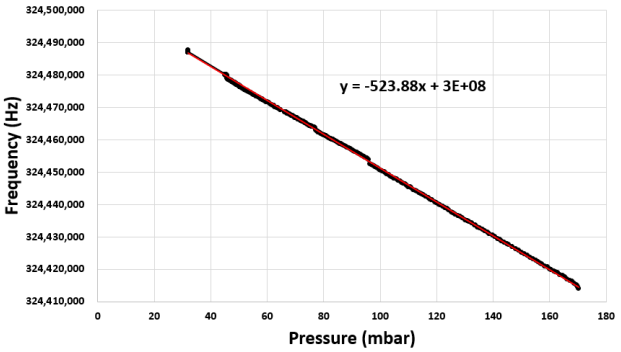

Figure 6: Pressure sensitivity measurement for a SSR1 cavity. The pressure sensitivity is -523.9 Hz/mbar for SSR1 VZ#2 jacket.

During the vertical test, quality factor along with X-ray radiation, LFD, and pressure sensitivity are measured.

CONCLUSION

We have conducted tests on the single-spoke resonator, specifically referred to as type 1 (SSR1), as part of the RAON SCL2 project. Design parameters for single-spoke resonators (SSRs) are provided, along with an analysis of their magnetic shielding effect. Magnetic shielding within the cryostat remains below 10 mG. The single-spoke resonator cavities, cryogenic systems, cryostats, and HMI are depicted for the vertical test setup. Performance evaluations of SSR1 superconducting cavities are carried out through vertical testing, revealing that the quality factor of two SSR1 cavities exceeds the reference value. Additionally, measurements of Lorentz force detuning (LFD) and pressure sensitivity are conducted on the SSR1 cavities.

REFERENCES

[1] H. Sakai *et al.*, "Field emission studies in vertical test and during cryomodule operation using precise x-ray mapping system", *Phys. Rev. Accel. Beams*, vol. 22, p. 022002, 2019. doi:10.1103/PhysRevAccelBeams.22.022002

[2] H. Kim, C.S. Park, S.J. Yu, "Generalized electron emission theory for one-dimensional conducting materials", *Appl. Sci.*, vol. 14, p. 2993, 2024. doi:10.3390/app14072993

[3] S. Jeon *et al.*, "Field emission and x-ray effect on RAON HWR superconducting cavity performance", *Curr. Appl. Phys.*, vol. 38, pp. 67-75, 2022. doi:10.1016/j.cap.2022.03.014

ISBN: 978-3-95450-247-9 ISSN: 2673-5490 doi: 10.18429/JACoW-IPAC2024-MOPC34

[4] J. Kim, H. Kim, "Quality Factor Measurement Method Using Multi Decay Time Constants on Cavity", in *Proc. 28th Linear Accelerator Conf. (LINAC'16)*, East Lansing, Michigan, USA, Sep. 2016, pp. 964-966. doi:10.18429/JACoW-LINAC2016-THPLR069

[5] H. Kim, "Conservation of quality factor for superconducting cavities and mammals under relativistic motion", *J. Korean Phys. Soc*., vol. 84, pp. 224-230, 2024. doi:10.1007/s40042-023-00961-0

[6] H. Kim, S. Jeon, Y. Jung, J. Kim, "Magnetic heating effect for Quarter-Wave Resonator (QWR) superconducting cavities", *Quantum Beam Sci.*, vol. 7, p. 21, 2023. doi:10.3390/qubs7030021

[7] H. Kim *et al.*, "Preparations of QWR cavities for beam commissioning", in *Proc. 14th International Particle Accelerator Conf. (IPAC'23)*, Venezia, IOP Publishing, Journal of Physics: Conference Series, vol. 2687, p. 082007, 2024. doi:10.1088/1742-6596/2687/8/082007

[8] C.M. Ginsburg, C. Reid, D.A. Sergatskov, "Magnetic Shielding for the Fermilab Vertical Cavity Test Facility", in *IEEE Transactions on Applied Superconductivity*, 2009, vol. 19, pp. 1419-1422. doi:10.1109/TASC.2009.2018234